

Superconducting $Sr_{0.85}La_{0.15}CuO_2$ bicrystal grain boundary Josephson junctions

**Victor Leca^{1,2,3}, Jochen Tomaschko², Di Wang⁴, Mihai Danila²,
Wim Arnold Bik⁵, Reinhold Kleiner¹, Dieter Kölle¹**

¹*Physikalisches Institut & Center for Collective Quantum Phenomena in LISA+, Universität Tübingen, Germany*

²*National Institute for Research and Development in Microtechnologies, Bucharest, Romania*

³*Faculty of Applied Chemistry and Materials Science, Polytechnique University of Bucharest, Romania*

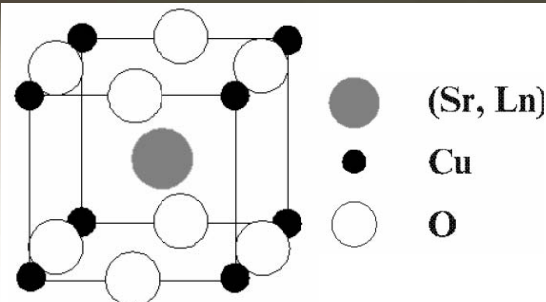
⁴*Karlsruher Institut für Technologie, Institut für Nanotechnologie, D-76021 Karlsruhe, Germany*

⁵*AccTec BV, TN/Cyclotrongebouw, Technische Universiteit Eindhoven, The Netherlands*

Outline

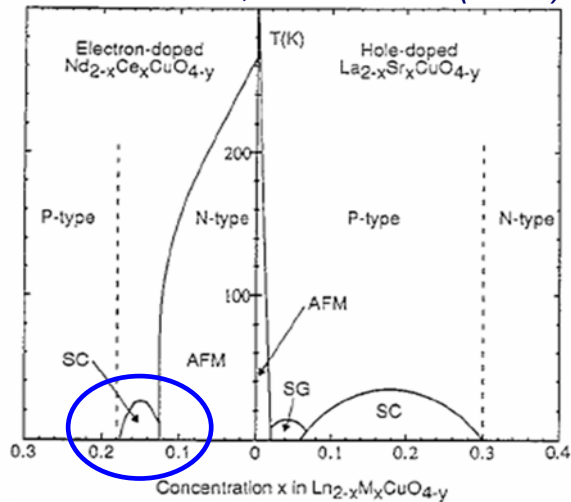
1. Motivation of the work - the electron-doped infinite-layer type $\text{Sr}_{1-x}\text{La}_x\text{CuO}_2$ high T_c superconductors
2. $\text{Sr}_{1-x}\text{La}_x\text{CuO}_2$ ($x=0.125-0.15$) thin films: PLD growth by the reduction method and characterization (RHEED, XRD, HRTEM, RBS)
3. Grain boundary $\text{Sr}_{1-x}\text{La}_x\text{CuO}_2$ ($x=0.15$) Josephson junctions
4. Conclusions

The $Sr_{1-x}La_xCuO_2$ (SLCO) compounds



$Sr_{1-x}Ln_xCuO_2$; $T_{c,max} = 43 K$
-infinite-layer type structure

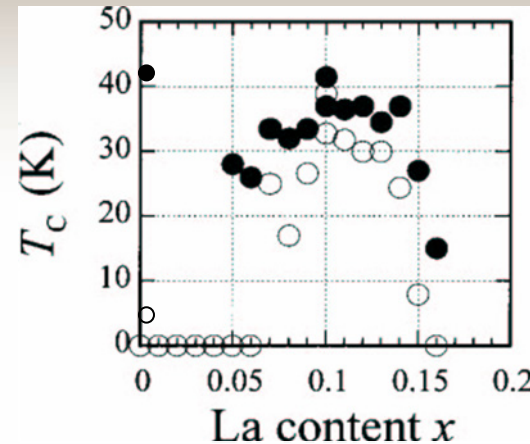
Smith et al., Nature 351 (1991)



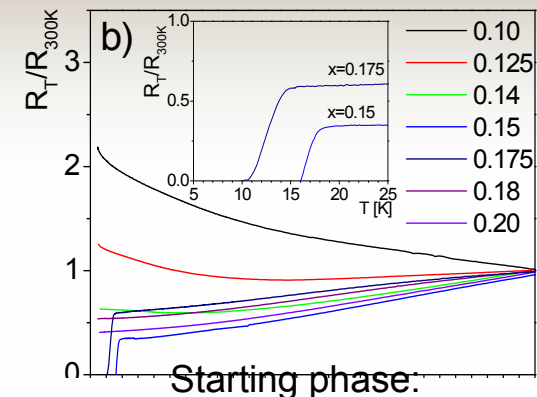
I_c vs. dopant concentration phase diagram for $T'-Ln_{2-x}Me_xCuO_4$

Optimum doping for SLCO?

MBE growth on (001) $KTaO_3$
(reduction method)

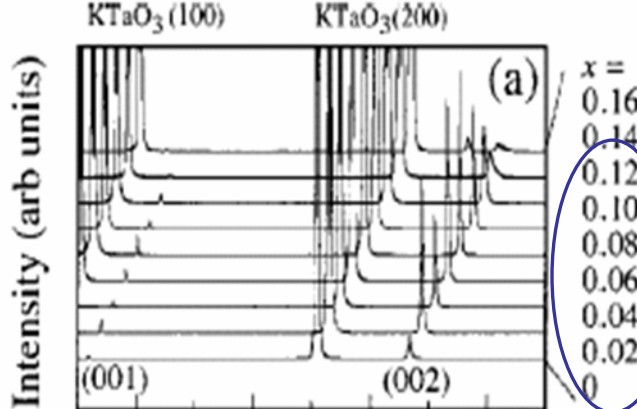


PLD growth on (001) $KTaO_3$
(oxidation method)



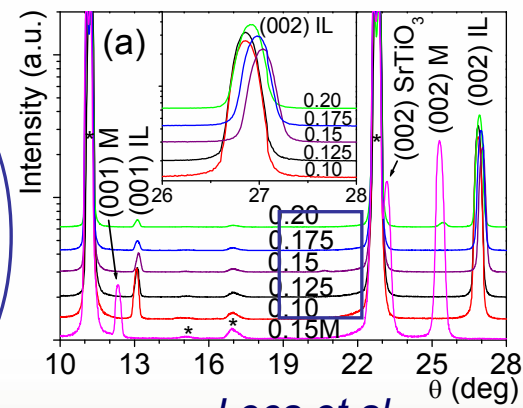
Starting phase:

$2\sqrt{2}a_p \times 2\sqrt{2}a_p \times c$ (super)structure



Karimoto et al.

Appl. Phys. Lett. 79 (2001)

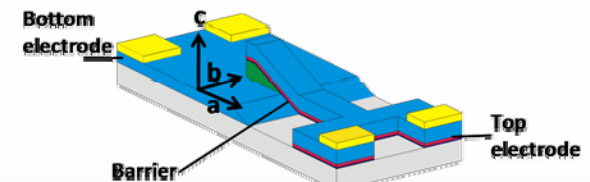
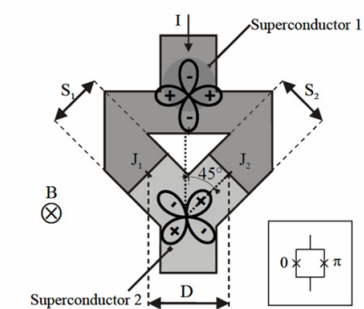
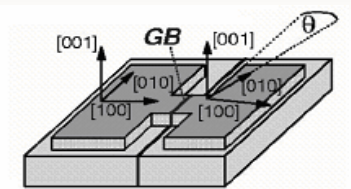
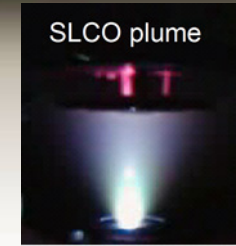


Leca et al.

Appl. Phys. Lett. 89 (2006)

Motivation of the work

1. Studies on the $\text{Sr}_{1-x}\text{La}_x\text{CuO}_2$ ($x=0.10-0.175$) thin films - *role of the epitaxial strain on structural and transport properties* for PLD grown films on different substrates: (001) SrTiO_3 , (001) KTaO_3 , and (110) DyScO_3
2. Transport properties of $\text{Sr}_{1-x}\text{La}_x\text{CuO}_2$ grain-boundary Josephson junctions
3. Studies on the *order parameter symmetry* – based on grain boundary Josephson junctions and phase sensitive experiments (on tetracystals, using 0- and π -SQUIDs) for different La doping levels ($x=0.10-0.175$) and temperatures ($2 \text{ K}-T_c$)
4. *Physics at the interface* between p- and n-type HTSc superconductors (based on ramp-type Josephson junction technology)



$Sr_{1-x}La_xCuO_2$ (0.125-0.15) growth parameters

On (001) $KTaO_3$ and (110) $DyScO_3$

$Sr_{1-x}La_xCuO_2$:

$T_d = 500\text{-}575^\circ C$

$P_d = 0.20\text{-}0.40$ mbar O_2

Post-deposition vacuum annealing
(reduction) @ 10^{-7} mbar:
- 15-20 min ($KTaO_3$ case)
- 20-30 min ($DyScO_3$ case)

**T_c : up to 24 K, on $KTaO_3$
up to 18 K, on $DyScO_3$**

Film's composition ($x_t=0.15$ target),
from RBS data:

- $x_f = 0.145$, films grown on $KTaO_3$
- $x_f = 0.135$, films grown on $DyScO_3$

On $BaTiO_3$ - buffered (001) $SrTiO_3$

$BaTiO_3$:

$T_d = 700\text{-}850^\circ C$

$P_d = 0.10$ mbar O_2

Post-deposition annealing:
- 15 min @ $950^\circ C$, under 0.10 mbar O_2 , and
30 min @ $950^\circ C$, in vacuum (10^{-7} mbar)

$Sr_{1-x}La_xCuO_2$:

$T_d = 550\text{-}600^\circ C$

$P_d = 0.20$ mbar O_2

Post-deposition annealing (reduction):
45-60 min @ $550^\circ C$, in vacuum (10^{-7} mbar)

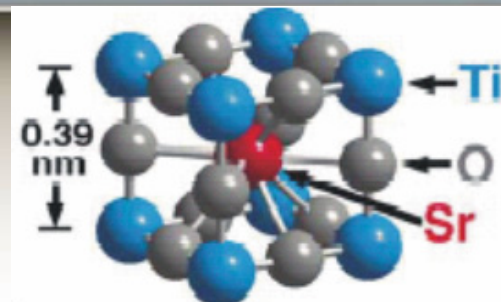
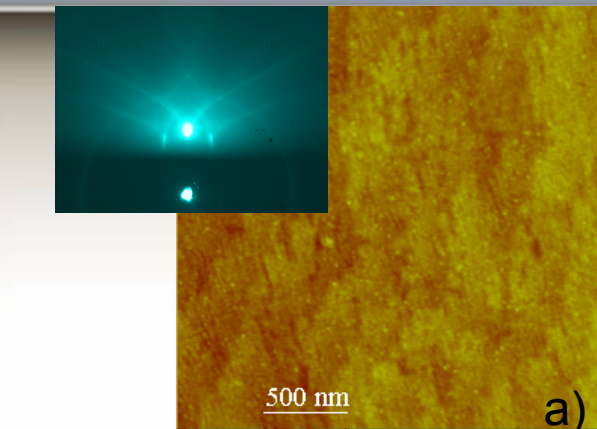
Film's composition ($x_t = 0.15$ target),
from RBS data: $x_f = 0.145$

T_c : up to 21 K

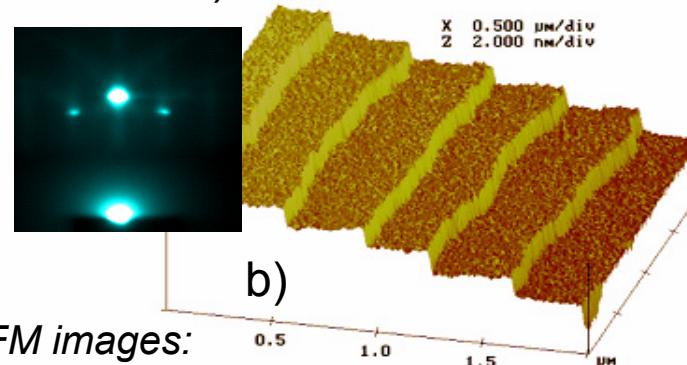
Highest reported T_c values for PLD grown SLCO films!

*Tomaschko, Leca, Selistrovski, Diebold,
Jochum, Kleiner, Koelle, Phys. Rev. B 85 (2012)*

Substrate morphology – SrTiO_3



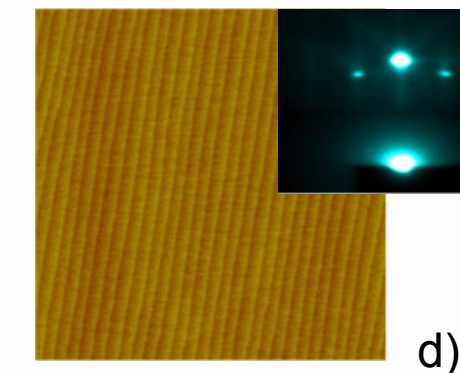
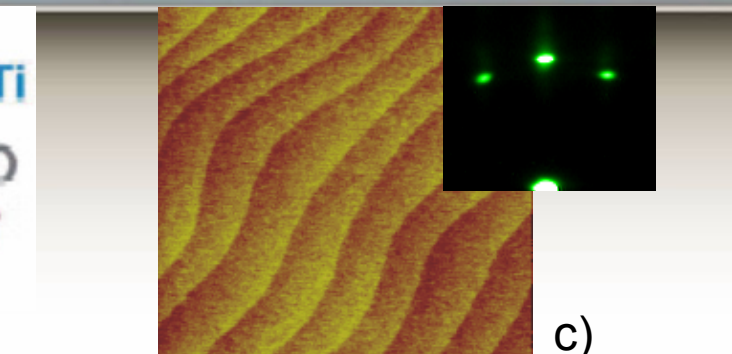
SrTiO_3 structure



RHEED and AFM images:

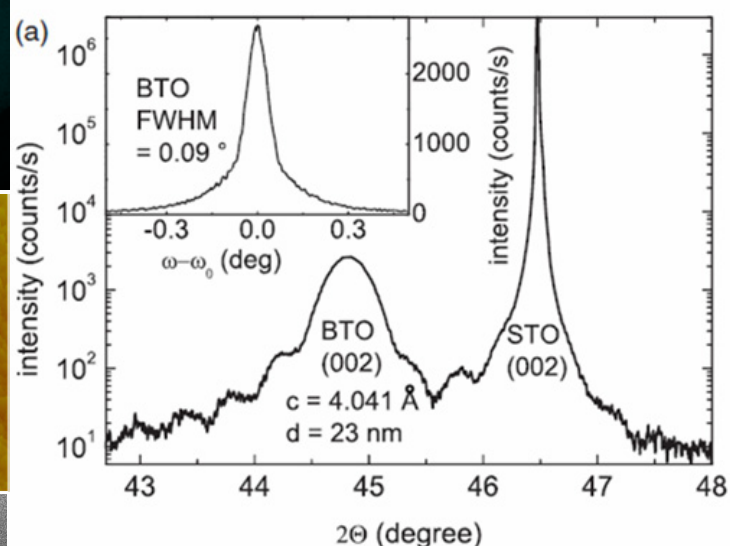
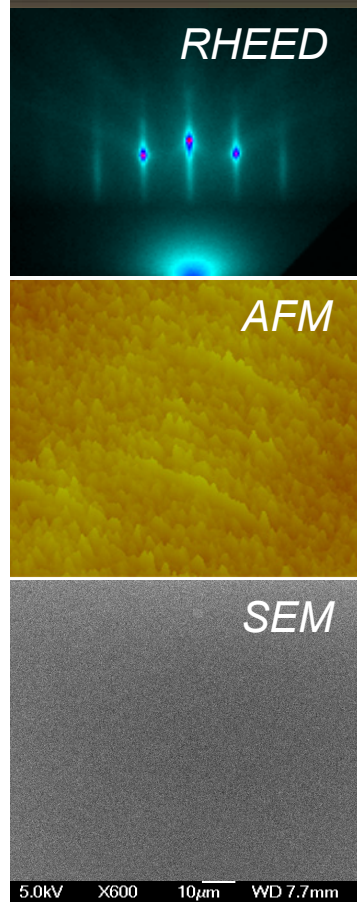
- a) of an as-received substrate
- b) after chemical treatment (BHF) and subsequent annealing ($950^\circ\text{C}/1\text{h}/\text{O}_2$) $\Rightarrow \text{TiO}_2$ termination
- c) after annealing ($950^\circ\text{C}/1\text{h}/\text{O}_2$) $\Rightarrow \text{SrO}$ termination
- d) after chemical treatment (BHCl) and subsequent annealing ($950^\circ\text{C}/1\text{h}/\text{O}_2$) $\Rightarrow \text{TiO}_2$ termination
(high miscut angle case)

Control of the surface termination by selective removal of one of the surface oxides.



Kawasaki et al. *Science* 226 (1994)
Koster et al. *Appl. Phys. Lett* 73 (1998)
Leca, PhD thesis (2003)

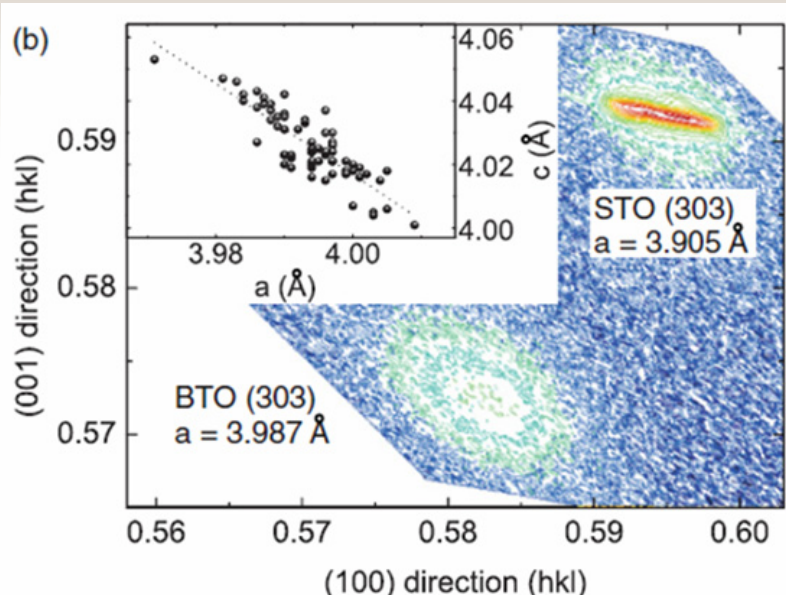
$Sr_{1-x}La_xCuO_2$ ($x=0.15$) grown on $BaTiO_3/SrTiO_3$ (001)



2θ/ω XRD scan of (002) BTO/STO

- single phase;
- epitaxial, c-axis oriented;
- tetragonal symmetry

The $BaTiO_3$ buffer layer



XRD rsm of (303) BTO/STO

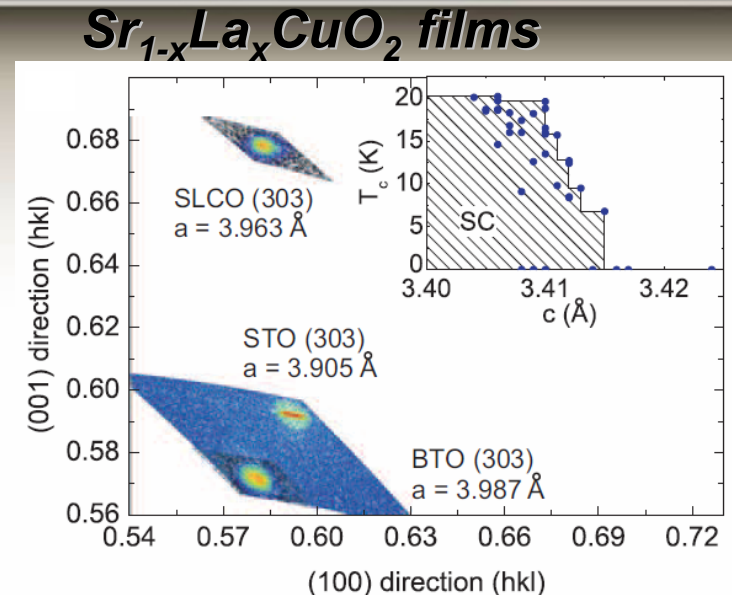
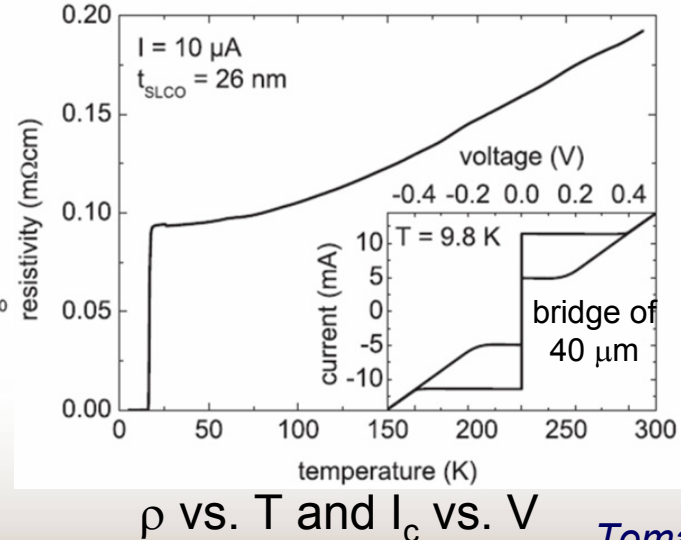
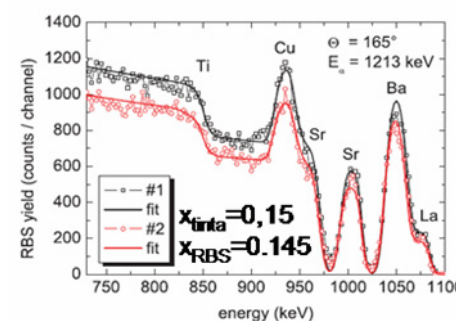
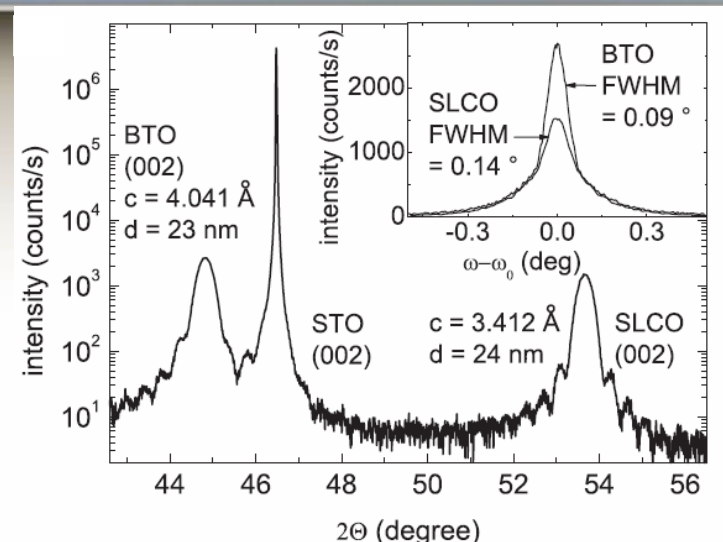
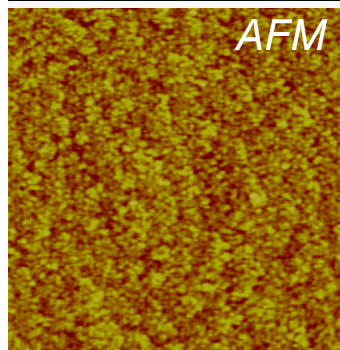
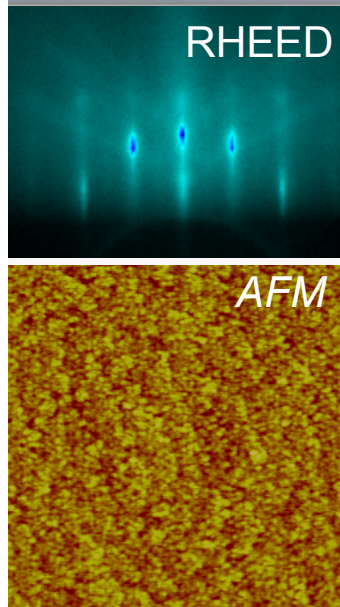
Smooth surface
for sharp interface

Deposition conditions for $BaTiO_3$:

$T_d = 750^\circ\text{C}$, $P_d = 0.10 \text{ mbar } O_2$, $E_d = 1.75 \text{ J/cm}^2$;
annealing 15 min/950°C/0.10 mbar O_2 and 30 min/950°C/10⁻⁷ mbar

Tomaschko, Leca, Selistrovski, Diebold,
Jochum, Kleiner, Koelle, Phys. Rev. B 85 (2012)

$Sr_{1-x}La_xCuO_2$ ($x=0.15$) grown on $BaTiO_3/SrTiO_3$ (001)

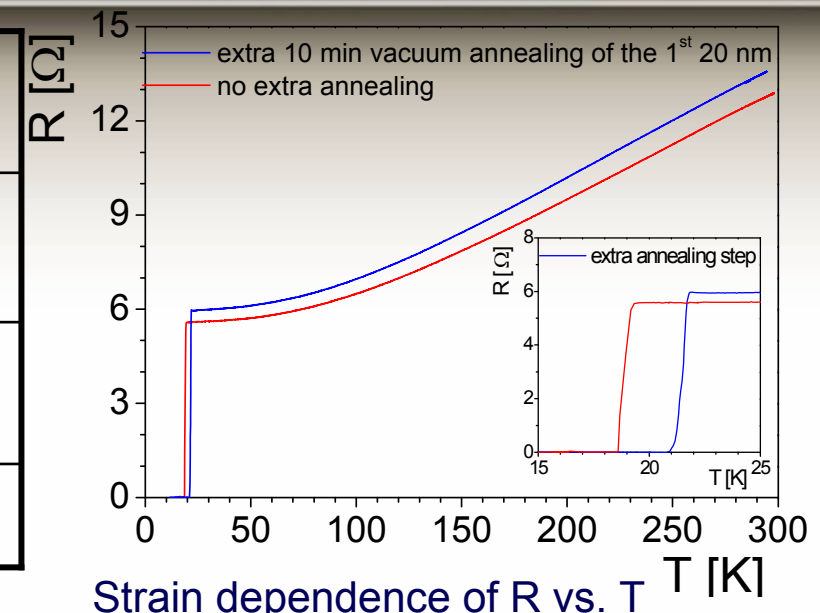
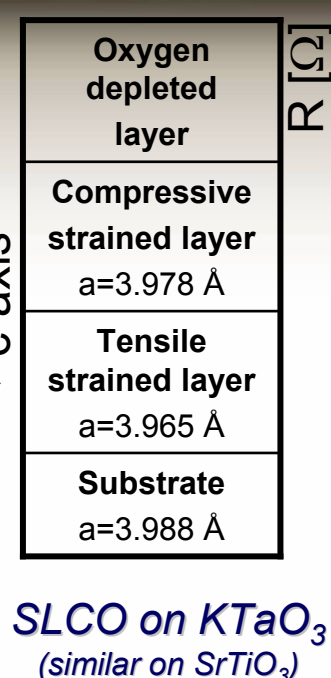
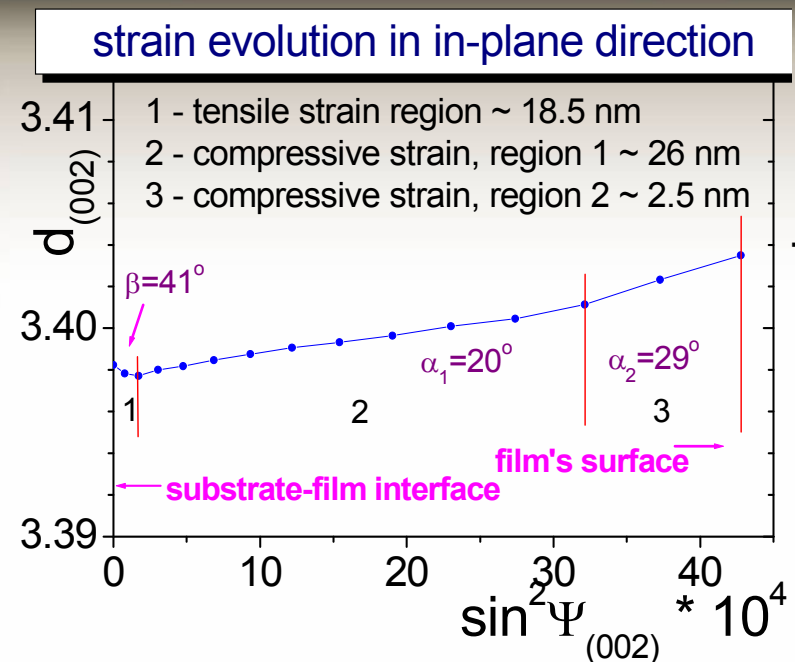


XRD rsm of (303) SLCO/BTO/STO

Deposition conditions:
 $T_d = 550^\circ C$, 0.20 mbar O_2 ;
 50 min/550°C/ 10^{-7} mbar
 $T_{c,0} = 12-21$ K
 $J_c@4.2K = 2.1 \times 10^6$ A/cm²

Tomaschko, Leca, Selistrovski, Diebold,
 Jochum, Kleiner, Koelle, Phys. Rev. B 85 (2012)

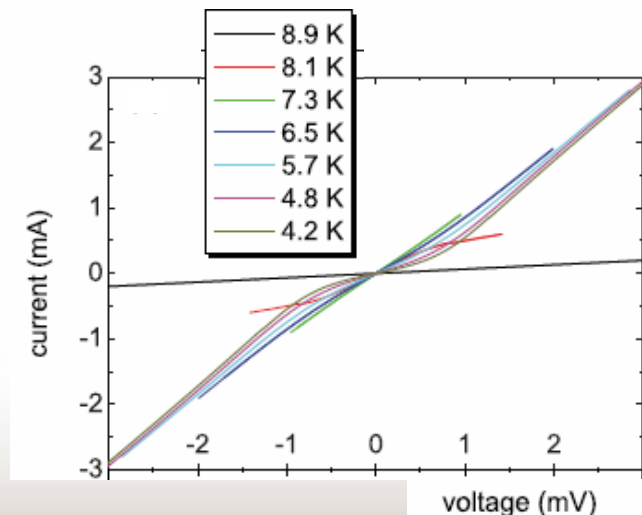
Role of the epitaxial strain



XRD and XPS: existence of an oxygen depleted top layer;

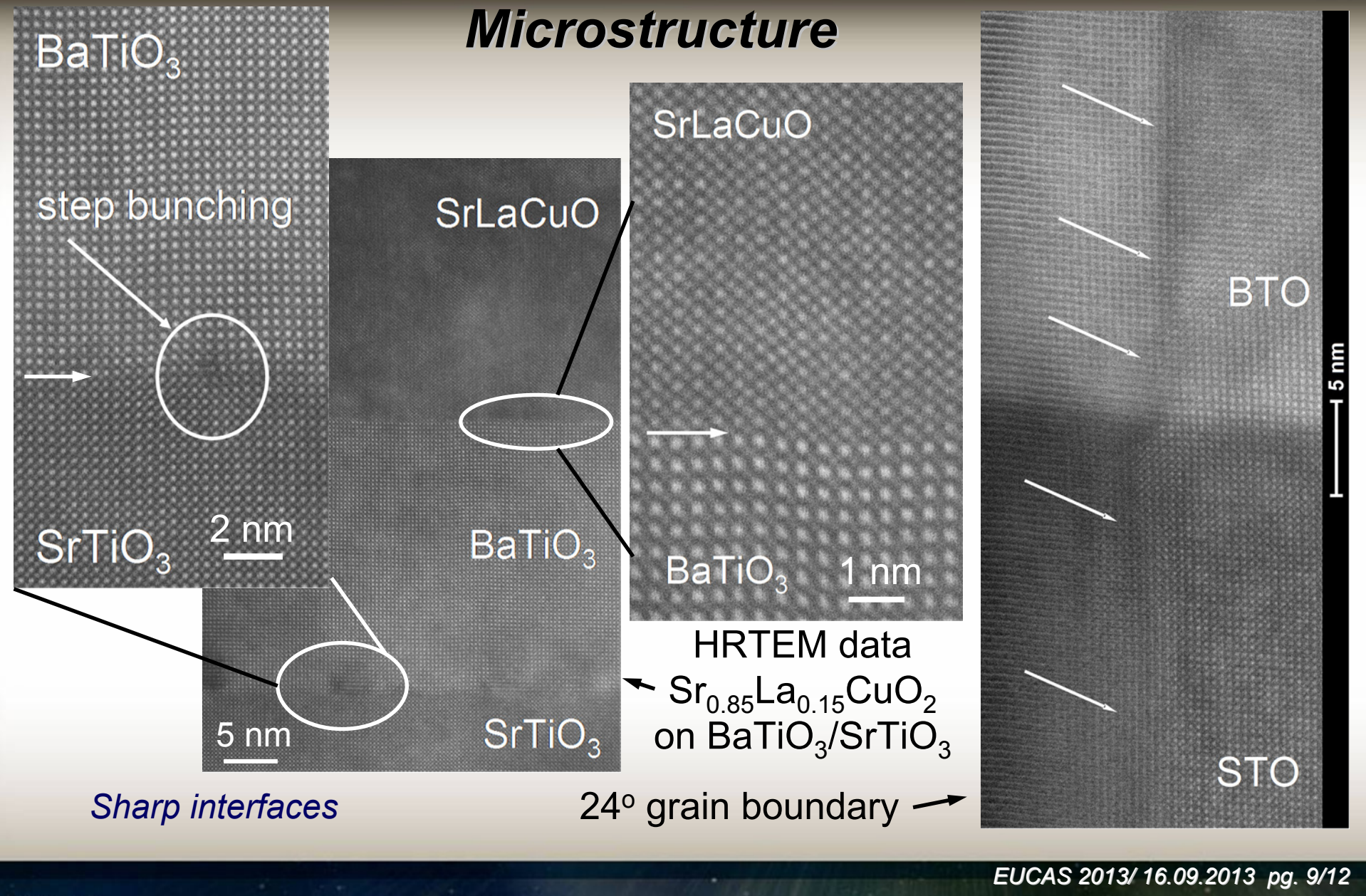
Implications: no Copper pair tunneling in planar SLCO/Au/Nb junctions

XRD: two types of strain: tensile (@ substrate-film interface) and compressive, on top

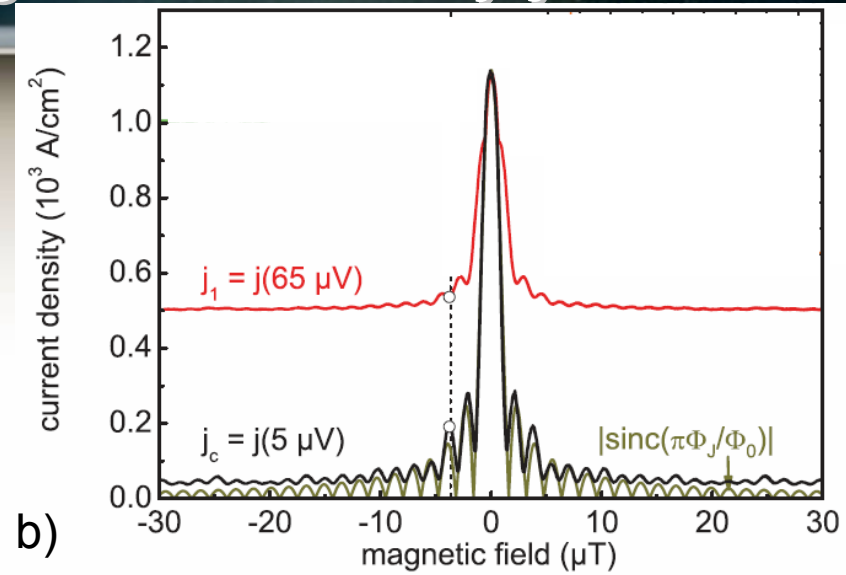
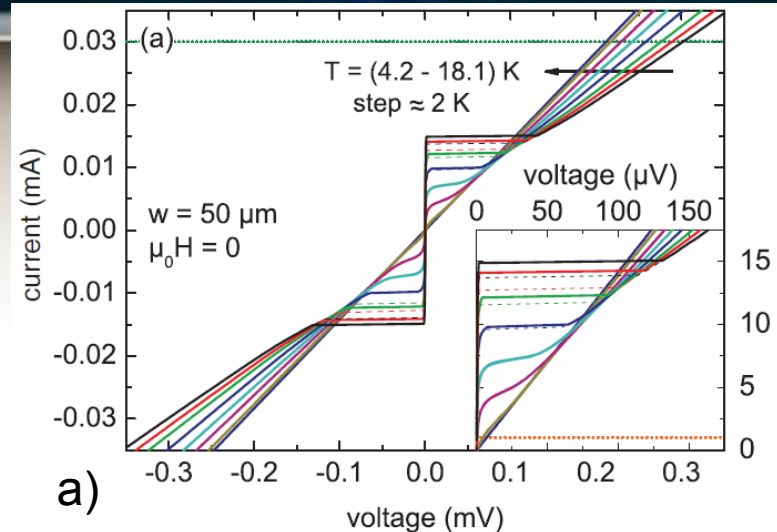


Tomaschko et al., PRB 84 (2011)

$Sr_{1-x}La_xCuO_2$ ($x=0.15$) grown on $BaTiO_3/SrTiO_3$ (001)



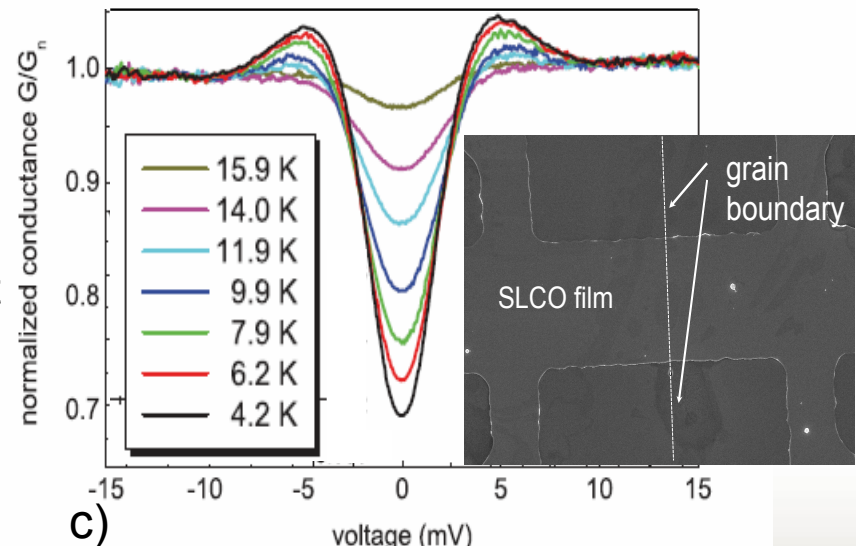
$Sr_{1-x}La_xCuO_2$ 24° symmetric grain boundary junctions



a) I-Vs: resistively and capacitively shunted junction (RCSJ)-like, with no significant excess current;
 $- J_c @ 4.2 \text{ K} \sim 1.2 \text{ kA/cm}^2$ – 1-2 orders of magnitude above J_c of 24° GB based on T' e-doped HTSc (NdCeCuO and LaCeCuO compounds)

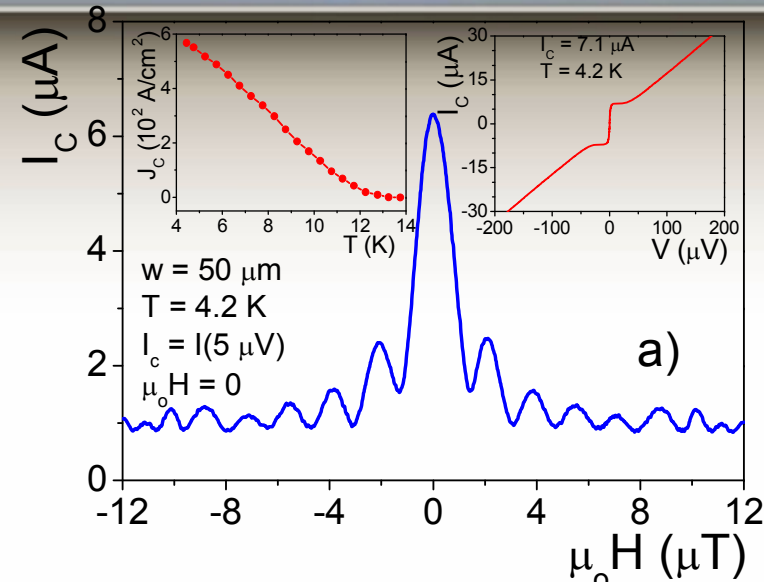
b) highly regular Fraunhofer-like patterns for different voltage criterion

c) conductance spectra did not show a zero-bias conductance peak. s-wave symmetry?
however, the V-shaped of the spectra in the subgap regime may indicate an order parameter with nodes

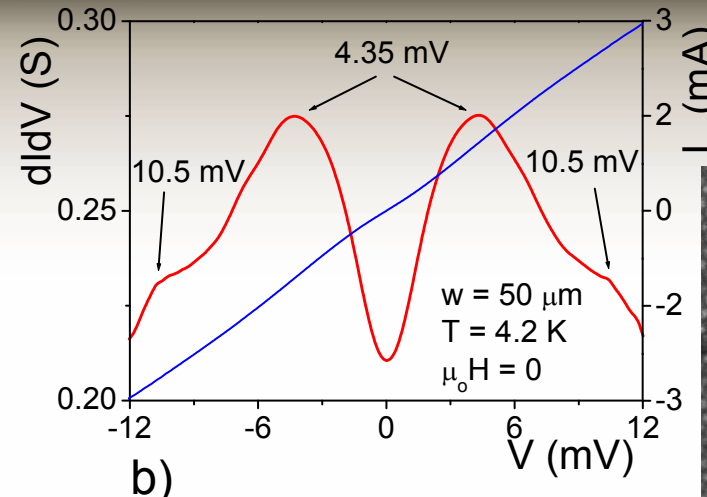


Tomaschko, Leca, Selistrovski,
Kleiner, Koelle, Phys. Rev. B 84 (2011)

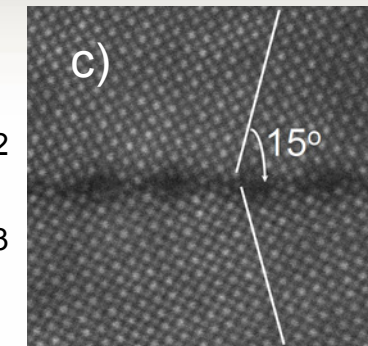
$Sr_{1-x}La_xCuO_2$ 30° symmetric grain boundary junctions



a)



b)



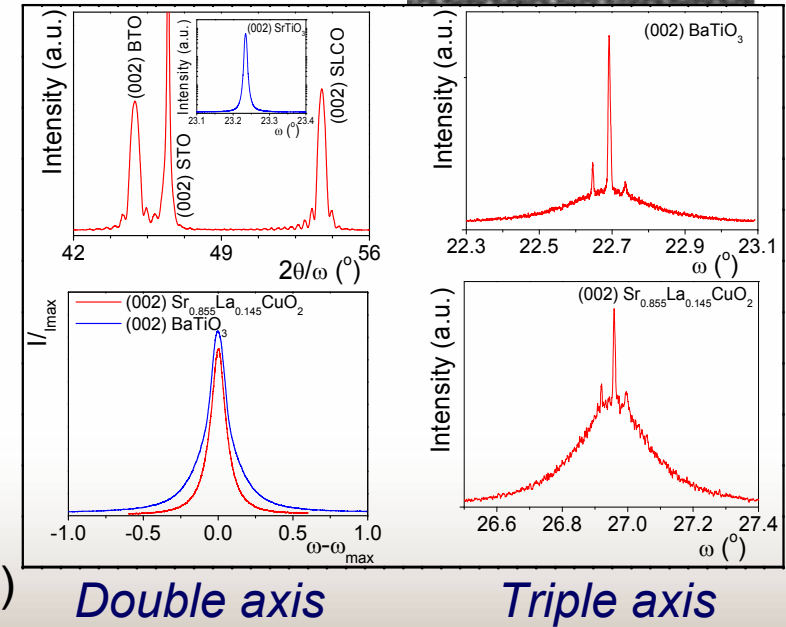
c)

- a) - I_c Vs: resistively and capacitively shunted junction (RCSJ)-like;
- highly regular Fraunhofer-like patterns;
- high J_c @ 4.2 K of $\sim 0.55 \text{ kA/cm}^2$; $I_c R_n$ of $\sim 50 \mu\text{V}$

b) conductance spectra did not show a zero-bias conductance peak (but a V-shaped subgap spectra, as for the 24° grain boundary junctions) **and** extra peaks above the coherence peaks; microscopic roughness?

c) plain view HRTEM of the substrate (30°) grain boundary;

d) XRD scans in double (one monochromator) and triple (two monochromators) axis configuration showing the presence of dislocations in the (buffer) BaTiO_3 and SLCO layers.

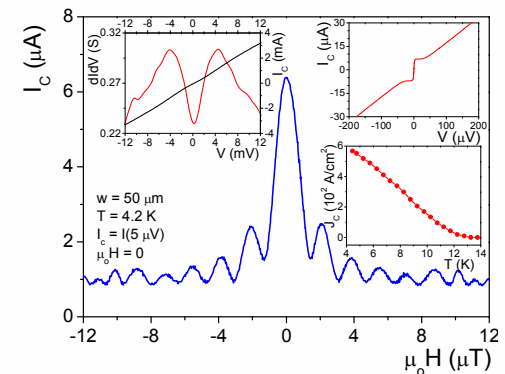
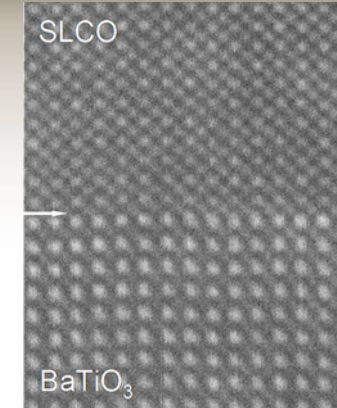


Double axis

Triple axis

Conclusions

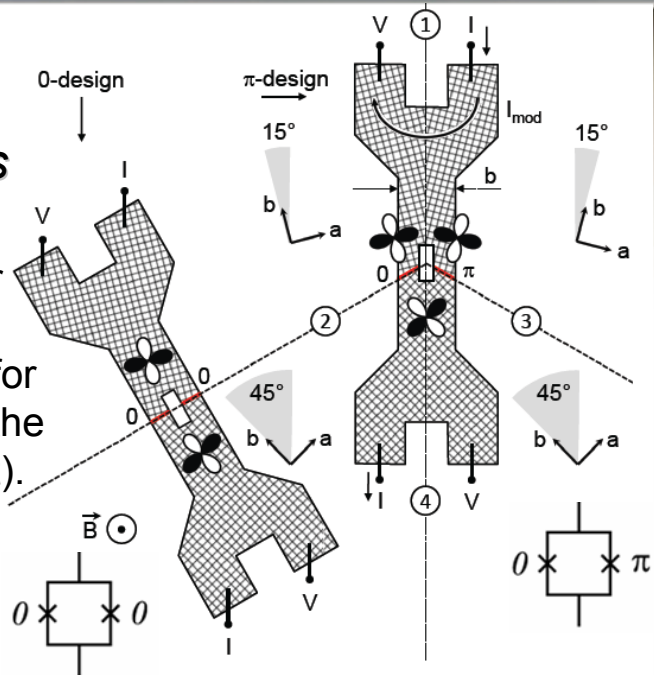
- the superconducting properties of the PLD grown electron-doped $\text{Sr}_{1-x}\text{La}_x\text{CuO}_2$ thin films are still far of those of the bulk or of the MBE grown films; however, higher phase stability could be achieved by PLD compared with other deposition techniques;
- epitaxial strain controls the structural and transport properties of the films; see the role of the substrate;
- first 24° and 30° [001] tilt grain boundary junctions were fabricated and their transport properties studied; no zero bias conductance peak was observed, probably due to strong disorder at the barrier (oxygen vacancies, etc).



Pairing symmetry from phase sensitive experiments

Schematic layout of the 0- and π -SQUIDs

- one grain boundary for the 0-SQUID;
- four grain boundaries for the π -SQUID (crossing the tetracystal central point).



For $d_{x^2-y^2}$ -wave symmetry: the π -SQUID consists of one 0-Josephson junction and one π Josephson junction (π -phase shift inside the SQUID loop).

Predominantly $d_{x^2-y^2}$ pairing symmetry

Tomaschko, Scharinger, Leca, Nagel, Kemmler,
Selistrovski, Koelle, Kleiner, Phys. Rev. B 86 (2012)

Chesca et al., PRL 90 (2003)
Schulz et al., APL 76 (2000)

I_c vs magnetic field for

a) 0- and b) π -SQUIDS

